Chapter 1

Sea-Floor Topography and Morphology of the Superswell Region

K. Jordahl · D. Caress · M. McNutt · A. Bonneville

1.1 Introduction

The islands of French Polynesia were discovered and populated by Polynesians between 500 B.C. and A.D. 500. European exploration of the region began in the seventeenth century. The main island groups (Society, Marquesas, Tuamotu, and Austral) have long been known, but the submarine topography has only been explored in the past fifty years using conventional echo sounders, and only in the past twenty years using higher-resolution multibeam sonar systems.

Better knowledge of sea-floor bathymetry in French Polynesia has been a priority for a number of reasons, both practical and scientific. To begin with, French Polynesia encompasses the Pacific's second largest Exclusive Economic Zone (EEZ), and certainly the world's largest EEZ per capita. Improved maps of the sub-sea topography are the first step to proper inventory of economic resources, including prime fishing grounds and submarine minerals, and accurate assessment of geologic hazards, including volcanic eruptions, tsunamis, and landslides (Auzende et al. 1997; ZEPOLYF 1996a, 1996b). In addition, the nature of the sea floor within French Polynesia has been of interest for a number of scientific reasons. For example, the area is unusually shallow for its age and contains an exceptional number of islands and seamounts that do not neatly fit into hotspot theory on account of anomalous trends or age progression (McNutt 1998; McNutt and Fischer 1987; McNutt and Judge 1990). A number of prominent tectonic lineations cross the region, providing information on relative plate motions and spreading center reorganizations (Cande and Haxby 1991; Jordahl et al. 1998).

Since the early 1990s, on average there have been three expeditions each year that have mapped the sea floor of French Polynesia using multibeam sonar systems (Fig. 1.1). The availability of these new data provides an excellent opportunity to create a new, up-to-date database of depth information for the sea floor in the central Pacific that can support a number of scientific studies and other practical uses.

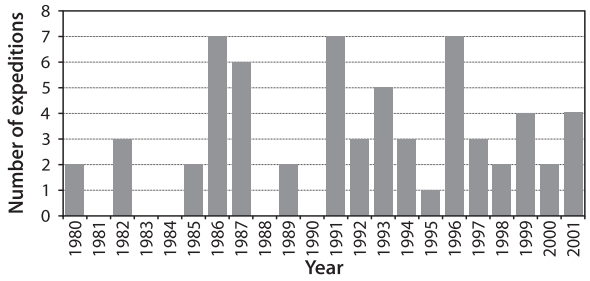

Fig. 1.1. Histogram showing number of multibeam expeditions per year to visit French Polynesia. Not all of these data sets were available for this analysis

Table 1.1. Institutions, ships, and multibeam systems

Institution	Ship	Multibeam system
France – Institut Français de Recherche pour l'Exploitation de la Mer (IFREMER)	N/O Jean Charcot N/O L'Atalante	Seabeam Simrad EM12D
Scripps Institution of Oceanography (SIO)	R/V Thomas Washington R/V Melville	SeaBeam SeaBeam 2000
Lamont-Doherty Earth Observatory (LDEO)	R/V Conrad R/V Maurice Ewing	SeaBeam Hydrosweep DS (through 2001)
USA – National Oceanic and Atmospheric Administration (NOAA)	R/V Surveyor R/V Discoverer	SeaBeam SeaBeam
Germany	F/S Sonne	SeaBeam
Japan Marine Science and Technology Center (JAMSTEC)	Kairai	SeaBeam 2112

Table 1.2. Expeditions used in the multibeam bathymetry compilation

Cruise	Institution	Year	Ship	Scientist
ETM19	IFREMER	1986	Charcot	Voisset
NIXO46	IFREMER	1986	Charcot	Voisset
NODCO1-1	IFREMER	1986	Charcot	Le Suavé
NODCO1-2	IFREMER	1986	Charcot	Voisset
NODCO2	IFREMER	1987	Charcot	Le Suavé
PAPNOUM	IFREMER	1987	Charcot	Foucher
RAPANUI2	IFREMER	1987	Charcot	Francheteau
SEAPSO5	IFREMER	1986	Charcot	Pontoise
SEARISE1	IFREMER	1980	Charcot	Francheteau
SEARISE2	IFREMER	1980	Charcot	Francheteau
TEAHITIA	IFREMER	1986	Charcot	Cheminée
FOUNDA	IFREMER	1997	L'Atalante	Maia
MANZPA	IFREMER	1999	L'Atalante	Dubois
NOUPA	IFREMER	1996	L'Atalante	Reyss
OLIPAC	IFREMER	1994	L'Atalante	Coste
PAPNOU99	IFREMER	1999	L'Atalante	Pelletier
POLYNAUT	IFREMER	1999	L'Atalante	Dubois
ZEPOLYF1	IFREMER	1996	L'Atalante	Bonneville
ZEPOLYF2	IFREMER	1999	L'Atalante	Bonneville
KR9912	JAMESTEC	1999	Kairei	–
ARIA01WT	SIO	1982	Washington	Shipley
ARIA02WT	SIO	1982	Washington	Lonsdale
CNXO01WT	SIO	1982	Washington	Robert (IFREMER)
PPTU03WT	SIO	1985	Washington	Mammerickx
CRGN01WT	SIO	1987	Washington	Winterer

Table 1.2. *Continued*

Cruise	Institution	Year	Ship	Scientist
CRGN02WT	SIO	1987	Washington	Natland/McNutt
CRGN03WT	SIO	1987	Washington	Cronan
RNDB16WT	SIO	1989	Washington	Guenther (transit)
TUNE01WT	SIO	1991	Washington	Tsuchiya
TUNE02WT	SIO	1991	Washington	Swift
TUNE03WT	SIO	1991	Washington	Talley
BMRG01MV	SIO	1995	Melville	Orcutt
BMRG02MV	SIO	1995	Melville	Lonsdale, Hawkins, Castillo
BMRG09MV	SIO	1995–1996	Melville	Lonsdale
WEST01MV	SIO	1993	Melville	Urabe (Geol. Surv. Japan)
WEST02MV	SIO	1993–1994	Melville	Lonsdale
WEST05MV	SIO	1994	Melville	Bryden
WEST12MV	SIO	1995	Melville	Moe
WEST13MV	SIO	1995	Melville	Coale
GLOR03MV	SIO	1992–1993	Melville	Forsyth
GLOR04MV	SIO	1993	Melville	Sandwell
GLOR05MV	SIO	1993	Melville	Sandwell
SOJN01MV	SIO	1996	Melville	*Transit*
SOJN02MV	SIO	1996	Melville	Chave
SOJN08MV	SIO	1997	Melville	*Transit*
SOJN09MV	SIO	1997	Melville	Chave
PANR05MV	SIO	1998	Melville	Hey
PANR06MV	SIO	1998	Melville	Gee
C2608	LDEO	1985	Conrad	Weissel
EW9102	LDEO	1991	Ewing	Detrick/Mutter
EW9103	LDEO	1991	Ewing	McNutt/Mutter
EW9104	LDEO	1991	Ewing	Larson
EW9106	LDEO	1991	Ewing	McNutt
EW9204	LDEO	1992	Ewing	McNutt
EW9205	LDEO	1992	Ewing	*Transit*
EW9602	LDEO	1996	Ewing	McNutt
EW9603	LDEO	1996	Ewing	*Transit*
EW0003	LDEO	2000	Ewing	*Transit*
RITS93B	NOAA	1993	Surveyor	Capt. F. J. Jones
RITS93C	NOAA	1993	Surveyor	Capt. F. J. Jones
RITS94A	NOAA	1994	Surveyor	Capt. Thomas Ruszala
DI9301	NOAA	1993	Discoverer	Capt. Robert Smart
TOGA92	NOAA	1992	Discoverer	Capt. Robert Smart
SO-47	Germany	1986	Sonne	Stoffers
SO-100	Germany	1995	Sonne	Devey
KR9912	–	–	–	–

1.2
Data Sources and Methods

We have assembled multibeam bathymetry from sixty-five oceanographic expeditions undertaken by research vessels from France, the United States, Germany, and Japan (Table 1.1). Table 1.2 lists the expeditions included in this compilation. Incorporation of these swath bathymetry data into a single map represents a significant challenge, in that they were collected by about half a dozen different sonar systems from various vendors and were archived in approximately two dozen different digital data formats. MB-System (Caress and Chayes 1996, 2003), an open source software package for the processing and display of swath mapping sonar data, is well suited for this sort of data compilation because of its modular and extensible i/o library. Most of the relevant formats were already supported, but in order to work with the French multibeam data it was necessary to create i/o modules for the raw Simrad EM12D format and the generic archival format (MBB) used by IFREMER (l'Institut Français de Recherche pour l'Exploitation de la Mer). Most of

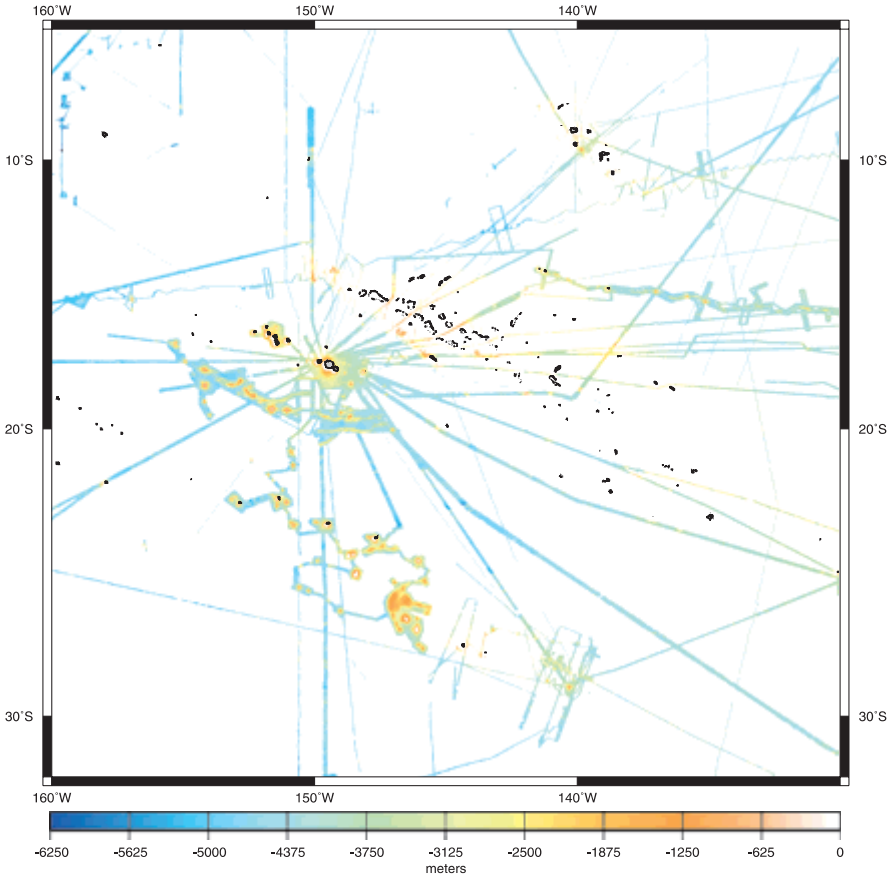

Fig. 1.2. New depth compilation for French Polynesia. Gaps between soundings have been left blank

the compiled multibeam bathymetry required little additional processing, but in a few cases interactive bathymetry and navigation editing removed significant artifacts.

Once the multibeam bathymetry database was in place, the data were used to create bathymetric grids using the MB-System. The full regional grids were produced at 1 km × 1 km resolution. In addition to the multibeam data, NGDC trackline data were included in gridding, as well as island topography from GTOPO30 and shoreline information from GSHHS (Wessel and Smith 1996). Soundings from the French Service Hydrographique et Océanographique de la Marine (SHOM) were also included, where they have been made available to the ZEPOLYF (Bonneville et al. 1995; Sichoix and Bonneville 1996) program (south of 10° S latitude).

Three separate small-scale grids were generated. The first contains data values only for grid nodes that are constrained by sonar bathymetry (Fig. 1.2) and provides an excellent representation of the true sonar coverage given the very different swath widths of the various multibeam systems. The other two grids used different strategies to fill the remaining grid nodes. Figure 1.3 was based entirely on thin-plate spline interpola-

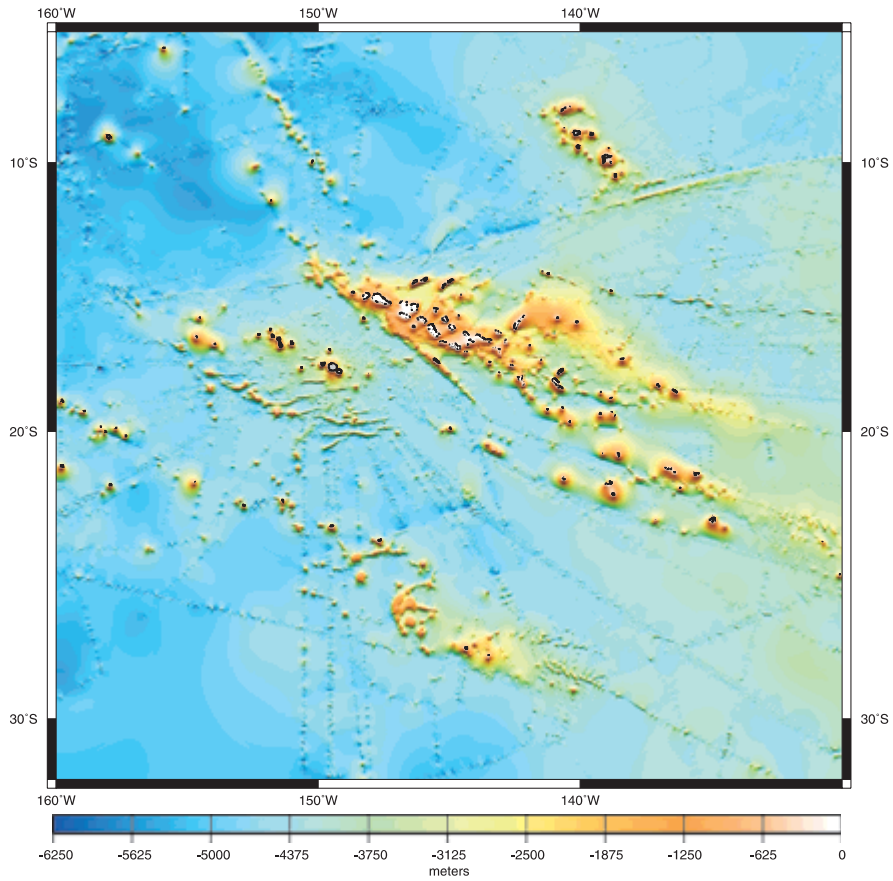

Fig. 1.3. New depth compilation for French Polynesia. Gaps between soundings were filled with spline interpolation

tion (Smith and Wessel 1990), while the final grid (Fig. 1.4) used predicted bathymetry from satellite altimetry (Smith and Sandwell 1994), incorporating the bathymetry from this database for both the long and the short wavelengths. The spline grid has the advantage of not including any data derived from gravity data, thus avoiding the problems of circular arguments in using the bathymetry grid for scientific studies that use both bathymetry and gravity as independent constraints to derive physical properties of the crust and mantle. Studies of lithospheric flexure, lateral variations in sediment thickness, sub-crustal intrusions, and subsurface loading would all be examples of studies that should not use bathymetry predicted from gravity. The spline grid is best in areas where ship track coverage is relatively dense, such as in the Society Islands. In other regions where gaps between the shiptracks can be on the order of 100 km (e.g., south of the Austral Islands), spline artifacts will degrade the utility of this grid for quantitative studies. In such areas, the predicted bathymetry grid (Fig. 1.4) provides the most accurate qualitative view of submarine features.

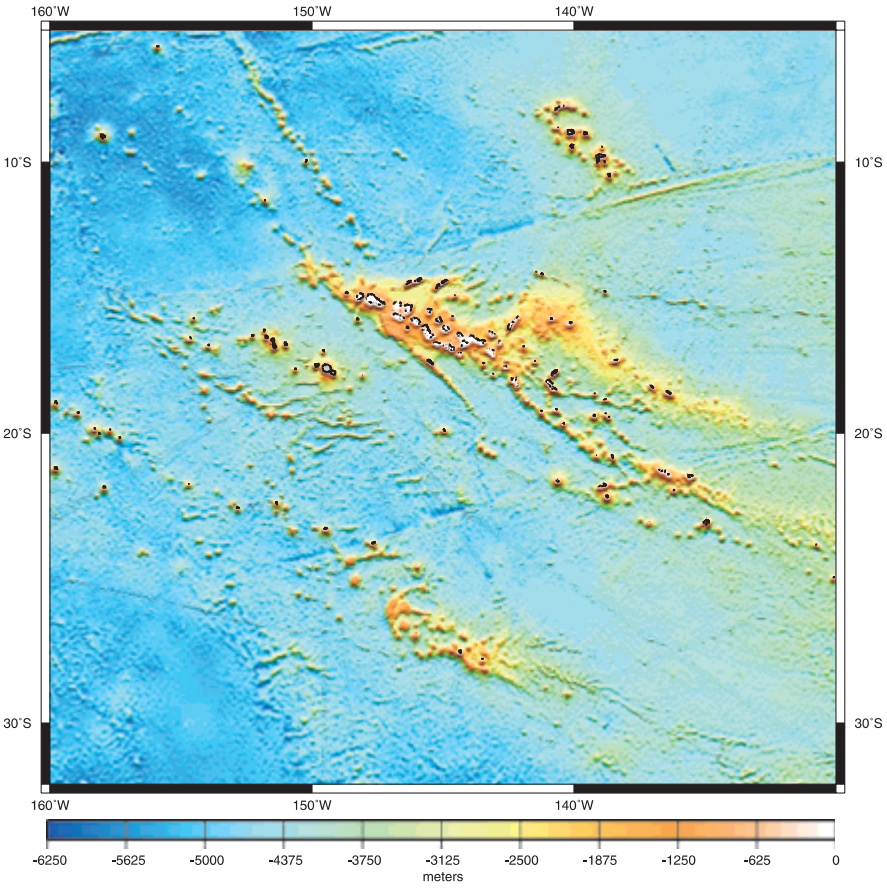

Fig. 1.4. New depth compilation for French Polynesia. Gaps between soundings were filled with depth predicted from satellite altimetry. In order to get a smooth blending between the two different data sets, their difference has been gridded (i.e., low-pass filtered) and then added to the predicted depth grid

There are a few artifacts seen in the grid that are emphasized by the illumination scheme used in Fig. 1.4. Most obvious is the pervasive "ringing" in the predicted bathymetry, where it is used to interpolate between ship soundings. This noise, with an average amplitude of ~100–200 m and spectral peak at ~50 km, is a side-lobe effect in the filtering scheme used to convert satellite altimetry to predicted bathymetry (Smith and Sandwell 1994). Other filtering schemes to suppress this noise would negatively impact the ability of the predicted bathymetry to resolve the positions and amplitudes of uncharted seamounts, and therefore this noise is tolerated.

A second type of artifact is a noticeable edge at the boundary between swaths of multibeam bathymetry and the base map. This effect is caused by local deviations between the multibeam depth and the regional average depth determined in the prediction scheme. The effect is enhanced by the differing resolutions inside versus outside the swaths.

In addition to viewing the sea-floor morphology of all of French Polynesia, this multibeam database allows us to grid the data on more local scales for a variety of purposes. For example, for small-scale morphological studies of seamounts and tectonic fabric, custom grids can be efficiently created at fine scale, because the database automatically reads only those files with soundings within the specified area of interest. The grids presented here are available via anonymous ftp from the server at ftp://ftp.mbari.org/pub/Polynesia.

1.3 Sea-floor Morphology in French Polynesia

Sea-floor depths in French Polynesia provide an excellent view of the morphology of the basaltic basement rocks on account of the low level of sedimentation, except locally near islands and shallow banks. For this reason, the bathymetry of French Polynesia has inspired a number of interpretations of sea-floor depth, ranging from regional studies of depth anomalies to fine-scale investigations of sea-floor fabric.

1.3.1 Bathymetric Expression of the Superswell

McNutt and Fischer (McNutt and Fischer 1987) first used the term "Superswell" to refer to the area in the south-central Pacific, largely coincident with French Polynesia, where the sea floor is several hundred meters to more than a kilometer shallower than typical for sea floor of the same geologic age elsewhere in the world's oceans. They noted that this area is also underlain by slow seismic velocities in the uppermost mantle (Nishimura and Forsyth 1985), has experienced an unusual volume of off-ridge volcanic activity, subsides more slowly than the global norm (Marty and Cazenave 1989), and appears to have an unusually weak lithospheric plate for its age at the time of volcanic loading based on flexure analysis (Calmant and Cazenave 1987). They argued that the South Pacific Superswell might have been unusually shallow for 100 million years or more, based on the fact that plate reconstructions place Menard's (1964) "Darwin Rise" over the same area of the mantle in the mid-Cretaceous. Menard had inferred a shallow depth for the Darwin Rise sea floor, currently located in the northwest Pacific, based on the elevation of the wave-cut summits of drowned former islands (guyots) above the surrounding sea floor.

McNutt and Judge (1990) identified an additional unusual feature of the Superswell: a geoid low corresponding to the topographic high. Cazenave and Thoraval (1993, 1994)

demonstrated that the seismic velocity anomalies in the upper mantle, geoid, and depth anomalies over the Superswell are all correlated at degree 6 spherical harmonic. Theoretical modeling at both labs demonstrated that the distinctive geoid/topography relationship of the Superswell could be explained by a broad dynamic upwelling of hot mantle material in a shallow low-viscosity zone beneath the region. However, the thermal anomaly in the upper mantle would not explain the unusually low values for elastic plate thickness reported for Superswell lithosphere (McNutt and Judge 1990). Therefore, any weakening of the elastic plate must be local to the island chains.

Levitt and Sandwell (1996) later questioned the existence of the South Pacific Superswell based on a modal analysis of newly collected multibeam bathymetry data from sea floor aged 15 to 35 Ma east of the French Polynesian hotspots. Their soundings were systematically deeper than the depths indicated in the older ETOPO5 gridded database (NGDC 1988) that had been used in the early studies to quantify the depth anomaly, leading them to question whether the Superswell might be an artifact of bad data. McNutt et al. (1996) re-examined the evidence for a large, regional depth anomaly spanning French Polynesia, confining the analysis to actual ship soundings. Their modal depth demon-

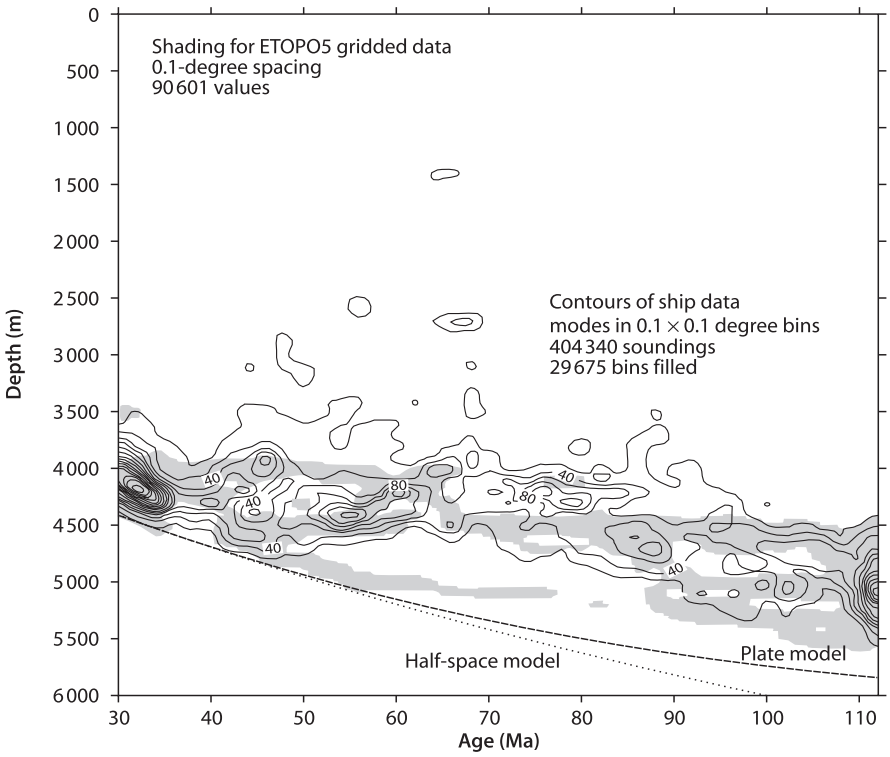

Fig. 1.5. Contour map of the mode of the depth/age relation for French Polynesia. The contour lines show the number of 0.1 × 0.1 degree latitude/longitude bins containing an original ship sounding that falls within each 100 m interval of depth and 2 Myr interval of age. Out of a total of 90 601 latitude/longitude bins, only about one third contain a ship sounding. Contour interval is 20 values beginning at 20. *Shading* represents the density of ETOPO5 values in the same bins, with contour interval 200 values starting at 100 (from McNutt et al. 1996)

strated remarkable agreement between the most up-to-date compilation of ship soundings and ETOPO5 in the depth/age relationship in French Polynesia, even though the number of ship soundings had increased fivefold since the release of ETOPO5 (Fig. 1.5).

The studies by Levitt and Sandwell (1996) and McNutt et al. (1996) highlight the importance of using actual depth soundings, rather than interpolated or predicted depths, in isolating depth anomalies. The new bathymetric map presented in Fig. 1.2 is based on a slightly augmented data set compared with what was available to McNutt et al. (1996) at the time, but it confirms the same general features of the Superswell. The depth anomaly grows from about 250 m on 30 Ma sea floor to approximately 1 000 m on 70–80 Ma lithosphere.

1.3.2 Midplate Swells

Broad (500–1 000 km) areas of elevated (500–2 000 m) sea floor typically surround regions of active intraplate volcanism (Crough 1978a,b, 1983). On account of their association with hotspots, these midplate swells have generally been interpreted as thermal in origin, either caused by altering the thickness/temperature in the lithosphere surrounding the hotspot (Detrick and Crough 1978; Detrick et al. 1981; McNutt and Judge 1990; McNutt 1987; Menard and McNutt 1982) or by the thermal buoyancy of a plume (Courtney and White 1986; Robinson and Parsons 1988a). One key observation in support of models that place at least some of the compensation for the swell as shallow as the mid to lower lithosphere is the ratio of the geoid anomaly to the depth anomaly, and thus accurate digital bathymetry maps have been important for constraining the origin of midplate swells.

In their broad survey of the heights and geoid-to-topography ratios of swells globally, Monnereau and Cazenave (1990) found that swell height increases and the geoid-to-topography ratio increases as the age of the lithosphere increases. Simple interpretation of the ratio in terms of a dipole compensation model would place the mass deficit supporting the swell in the mid to lower lithosphere, in apparent agreement with the lithospheric reheating model for midplate swells. However, theoretical models with realistic physical parameters had difficulty explaining the rapid rise time of midplate swells on account of the low coefficient for thermal conduction of the lithosphere. In comparison, swells surrounding hotspots in the South Pacific are generally smaller and have lower geoid-to-topography ratios than the global norm for hotspots elsewhere on lithosphere of the same age (Fig. 1.6), and therefore even shallower apparent compensation depths. Thus, the difficulty in supplying enough heat at shallow enough depth in the lithosphere to explain the low geoid-to-topography ratios is even more pronounced for the hotspots of the South Pacific.

More recent investigations have pointed out that melting models would predict a chemical component to swell relief as well as a thermal component (Jordan 1979). The extraction of a basaltic melt from more fertile mantle leaves a residuum depleted in aluminum and other elements that form the dense mineral garnet below 40–60 km depth. Therefore, the residuum is lighter than the undepleted mantle, potentially providing buoyancy to support a midplate swell depending on the viscosity and dynamic evolution of the depleted layer. For example, the depleted residuum might flow within the lower lithosphere to widths of hundreds of kilometers around the site of surface volcanism, thus matching the width of midplate swells (Phipps Morgan et al. 1995). On the other hand, it could spread more

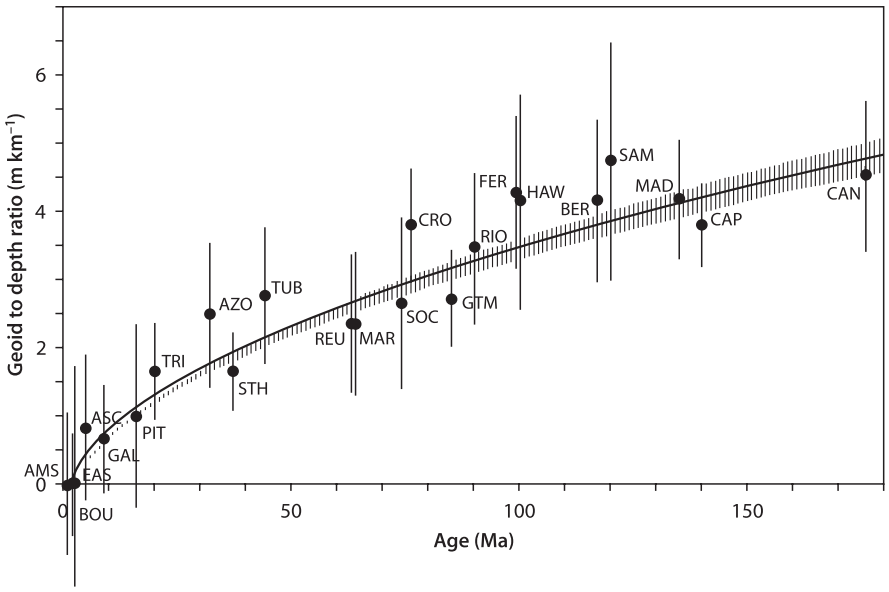

Fig. 1.6. Geoid-to-topography ratios as a function of age computed from swell height and geoid anomaly over hotspot swells. The *solid line* is the best fitting square root of age function. Note that all of the examples from the South Pacific such as Easter (EAS), Pitcairn (PIT), Marquesas (MAR), and Society (SOC) fall below the global trend, with the exception of Tubuai (TUB) (from Monnereau and Cazenave 1990)

uniformly over an even larger region, potentially halting the square-root-of-age subsidence of old oceanic lithosphere, particularly in the western Pacific. One advantage of providing at least a portion of the compensation for swell by chemical depletion is that it would have a shallow source, thus explaining the low geoid-to-topography ratios for swells without requiring substantial reheating of the lithosphere.

The observation from seismic reflection and tomographic studies that the crust immediately beneath several island chains is underlain by a presumably magmatic body lighter than the surrounding mantle offers another source for the buoyancy of swells. McNutt and Bonneville (2000) demonstrated that a seismically imaged body underplating the Marquesas Islands (Caress et al. 1995) has sufficient buoyancy to explain both the depth and the geoid anomaly over the Marquesas swell (Fig. 1.7). Bonneville and McNutt (to be published) are applying this same approach on the new bathymetric data from this paper to show that the Society and Austral swells could also have a similar origin, although the seismic tomography data for those island chains is not of sufficient quality to determine whether such underplating indeed exists. These recent investigations point out the importance of correcting for all shallower sources of anomalous crustal structure before attributing the rise of midplate swells to deeper sources.

1.3.3
Plate Boundary Features

The new bathymetric map for French Polynesia displays a number of features that record the history of plate boundaries in the South Pacific: fracture zones, abyssal hill

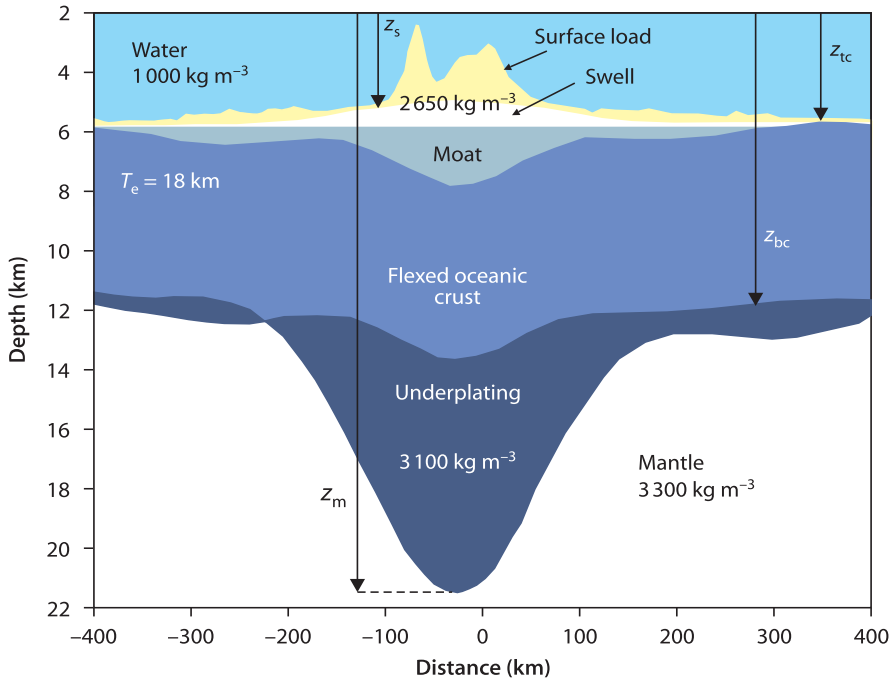

Fig. 1.7. Model for the Marquesas swell based on geophysical data from a line through the center of the chain. Only that portion of the bathymetric load above the swell is supported by elastic flexure. The swell itself is compensated by underplating. The shape of the underplating is consistent with seismic refraction data, and the depth of the moat agrees with seismic reflection data. Depths to the top of the swell, the top of the oceanic crust, the bottom of the oceanic crust, and the bottom of the underplating are indicated by *zs*, *ztc*, *zbc*, and *zm*, respectively. The small geoid-to-topography ratio results from the fact that the compensation for the swell is chemical rather than thermal and is indeed shallow (from McNutt and Bonneville 2000)

fabric, and the ancient traces of triple junctions and propagating rifts. Because some of the sea floor in this region was created during the Cretaceous superchron, such bathymetric features provide crucial evidence for past relative plate motions. Using actual bathymetry provides a substantial improvement over tectonic studies based on satellite altimetry (Okal and Cazenave 1985) on account of the higher resolution in sonar data and the fact that many of the plate boundary features are nearly isostatically compensated, and thus they have only a small signature in the altimetric geoid. For example, Kuykendal et al. (1994) used high-resolution, digitized locations of the Marquesas fracture zone from multibeam sonar to detect two subtle but important changes in Pacific-Farallon plate motion, the earlier one at 65–85 Ma (large uncertainty on account of lack of magnetic isochrons) and the more recent one between 33 and 37 Ma. The Pacific-Farallon ridge responded to a major change in the pole of rotation at about 50 Ma through the creation of a propagating rift, the trace of which has also been detected and interpreted in this data set (Cande and Haxby 1991; Jordahl et al. 1997; Jordahl et al. 1998).

Fracture zones have also been proposed as potential indicators of the strength of lithospheric plates by observing the magnitude of flexure that develops across frac-

ture zones as the opposing plates subside at different rates depending on the age difference across the fault (Sandwell and Schubert 1982). Most studies have relied on geoid profiles recovered from satellite altimetry to determine the flexural signal from a locked fault (Sandwell 1984; Sandwell and Schubert 1982; Wessel and Haxby 1990). However, a detailed study of the bathymetry along the large-offset Marquesas Fracture Zone (Jordahl et al. 1995) demonstrated that conclusions drawn from geoid studies alone can be in error, particularly if the section of the fracture zone being used was inside the active section of the transform fault during a time when the pole of rotation was shifting. In that case, the fine-scale details concerning the formation of intra-transform relay zones and propagating rifts as the transform adjusts to a new direction of spreading are not observed in the smooth geoid data. Estimates of the fault strength based on geoid analysis incorrectly indicate a weak fault unless high-resolution bathymetry data are available to sort out the details of transform adjustments. The new map presented in Fig. 1.2 includes some high-resolution crossings of the Austral Fracture Zone that could be useful for this sort of study.

1.3.4
Off-Ridge Features

One of the most distinguishing features of the Pacific Plate in the region of Polynesia is the large volume of off-ridge volcanism in forms ranging from linear, age progressive chains of large islands and seamounts (Duncan and McDougall 1974; Duncan and McDougall 1976; Bonneville et al. 2002) to discontinuous subparallel ridges (Sandwell et al. 1995; Winterer and Sandwell 1987) to an unusually large number of isolated seamounts (Bemis and Smith 1993). The pattern of volcanism is far from random even on casual inspection. Clearly the new map presented here, by displaying what has been observed for small-scale features within the large framework, has great potential for leading to new insights on what process or processes have led to this large volume of off-ridge volcanism and whether properties associated with the lithosphere (e.g., thickness, rigidity, state of stress, pre-existing fabric, etc.) have interacted with the melt source to create the variety of volcanic expressions (ten Brink 1991; Vogt 1974).

High-resolution bathymetry reveals a variety of morphologies amongst the Polynesian volcanoes. The most common morphology is a circular or oval seamount with

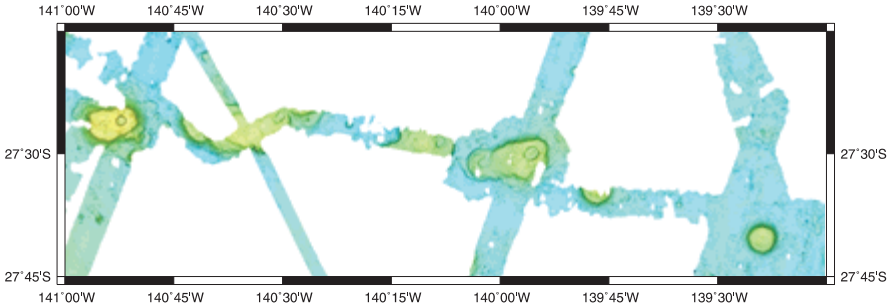

Fig. 1.8. Bathymetry of the Taukina Seamount chain in the south Austral region. The Taukina Seamounts are flat-topped, steep sided cones, 6–10 km in diameter and 1000–1500 m high. The Hydrosweep DS multibeam bathymetry is shown using a 100 m grid interval and shading by slope magnitude

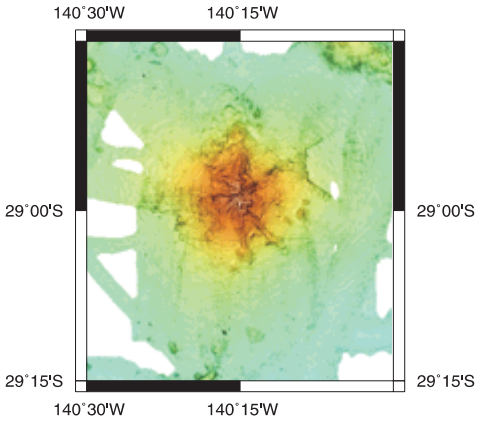

Fig. 1.9. Bathymetry of Macdonald Seamount in the south Austral region. This volcanically active seamount rises 3000 m above the surrounding sea floor. The SeaBeam and Hydrosweep DS multibeam bathymetry is shown using a 100 m grid interval and shading by slope magnitude

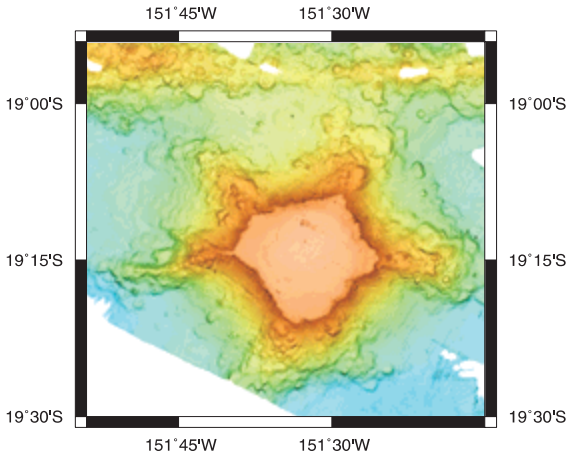

Fig. 1.10. Guyot Zep17 in the Tarava Seamounts south of the Society Islands is another example of a rift zone volcano (Clouard et al. 2003). The Simrad EM12D multibeam bathymetry is shown using a 100 m grid interval and shading by slope magnitude

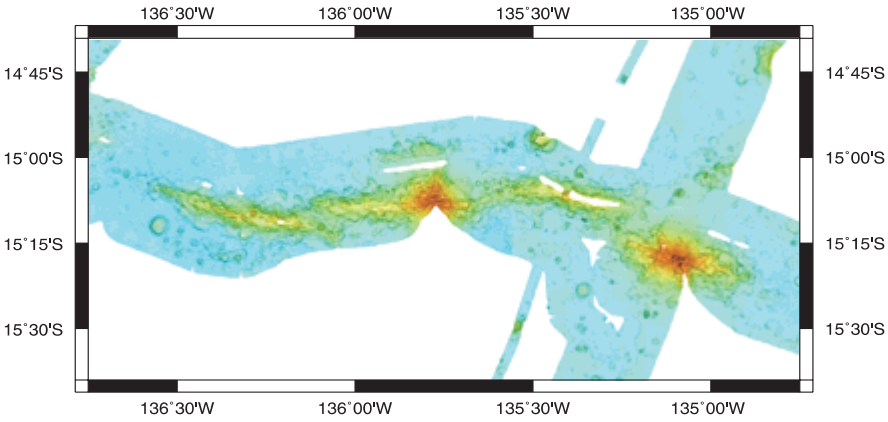

Fig. 1.11. Bathymetry of a segment of the Puka Puka Chain (Sandwell et al. 1995). These volcanic ridges are clearly constructed by the superposition of many small, flat-topped volcanic cones. The SeaBeam multibeam bathymetry is shown using a 100 m grid interval and shading by slope magnitude

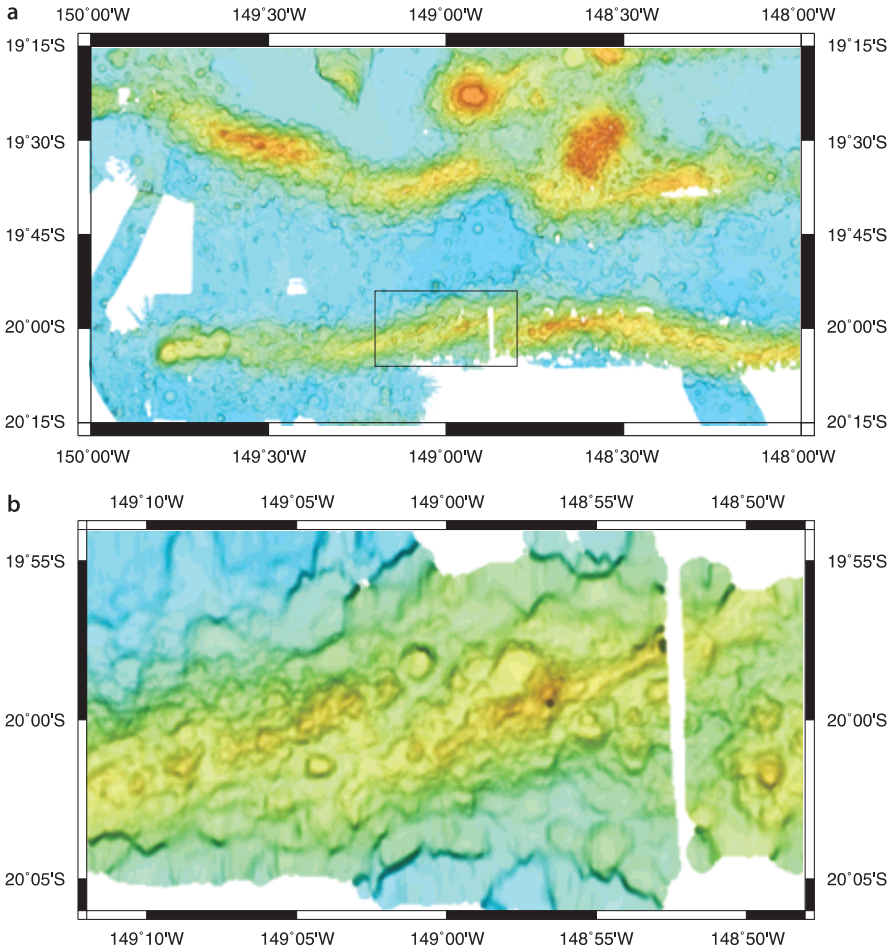

Fig. 1.12. a Bathymetry of a segment of the Va'a Tau Piti Ridges near Tahiti (Clouard et al. 2003). These volcanic ridges are clearly constructed by the superposition of many small, flat-topped volcanic cones. The Simrad EM12D, Hydrosweep DS and SeaBeam multibeam bathymetry is shown using a 100 m grid interval and shading by slope magnitude. **b** Detail of volcanic morphology of ridges in region shown by box in **a**

steep sides and flat tops, often with a prominent caldera (Scheirer et al. 1996). Most of the smaller seamounts have this form. Figure 1.8 shows examples from the Taukina Chain in the south Austral region that are 6–10 km across and 1 000–1 500 m high.

Many of the larger volcanoes develop linear zones of weakness emanating from a central peak. The tendency for magma to migrate along and erupt from these rift zones produces prominent radial ridges (Binard et al. 1991; see Sect. 5.1). Two fully mapped examples of these rift zone volcanoes are shown here: the Macdonald Seamount of the south Austral Chain in Fig. 1.9 (McNutt et al. 1997) and Guyot Zep17 in the Tarava Seamounts south of the Society Islands (Clouard et al. 2003) in Fig. 1.10.

Figures 1.2–1.4 show that en échelon volcanic ridges are also quite common in Polynesia. These ridges have been mapped in detail in the Puka Puka Chain (Fig. 1.11)

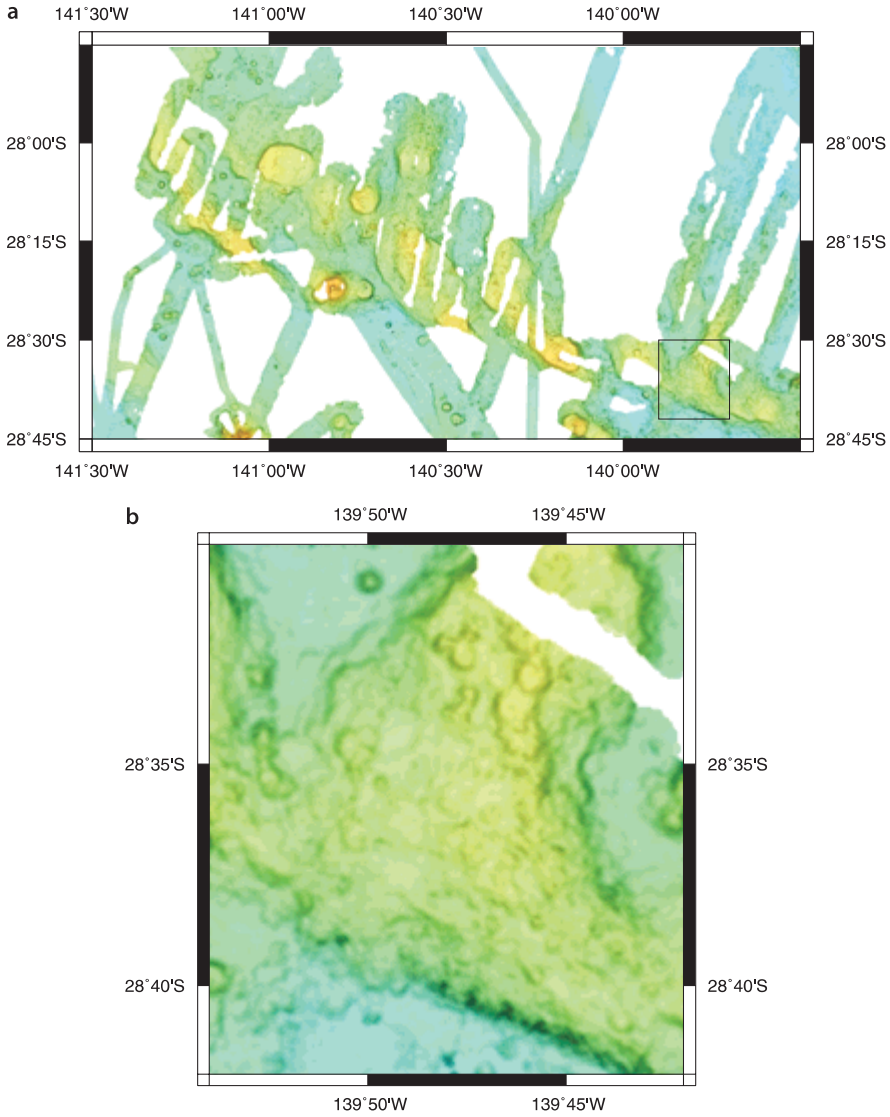

Fig. 1.13. a Bathymetry of the Ngatemato Seamount chain in the south Austral region. The Ngatemato Chain is mostly constructed of many small cones, like the Puka Puka and Va'a Tau Piti Ridges, but also includes some large, flat-topped edifices. The Hydrosweep DS, SeaBeam and Simrad EM12D multibeam bathymetry is shown using a 100 m grid interval and shading by slope magnitude; **b** detail of volcanic morphology of ridges in region shown by box in **a**

(Sandwell et al. 1995), the Austral Islands (McNutt et al. 1997) and the Va'a Tau Piti Ridges near Tahiti (Clouard et al. 2003), as seen in Fig. 1.12a,b. These ridges have generally been formed on young (<20 Ma) lithosphere and span scales from tens to hundreds of kilometers, possibly including entire island chains (e.g., the Tuamotu). High-resolution bathymetry reveals that these ridges are actually constructed of many small, flat-topped

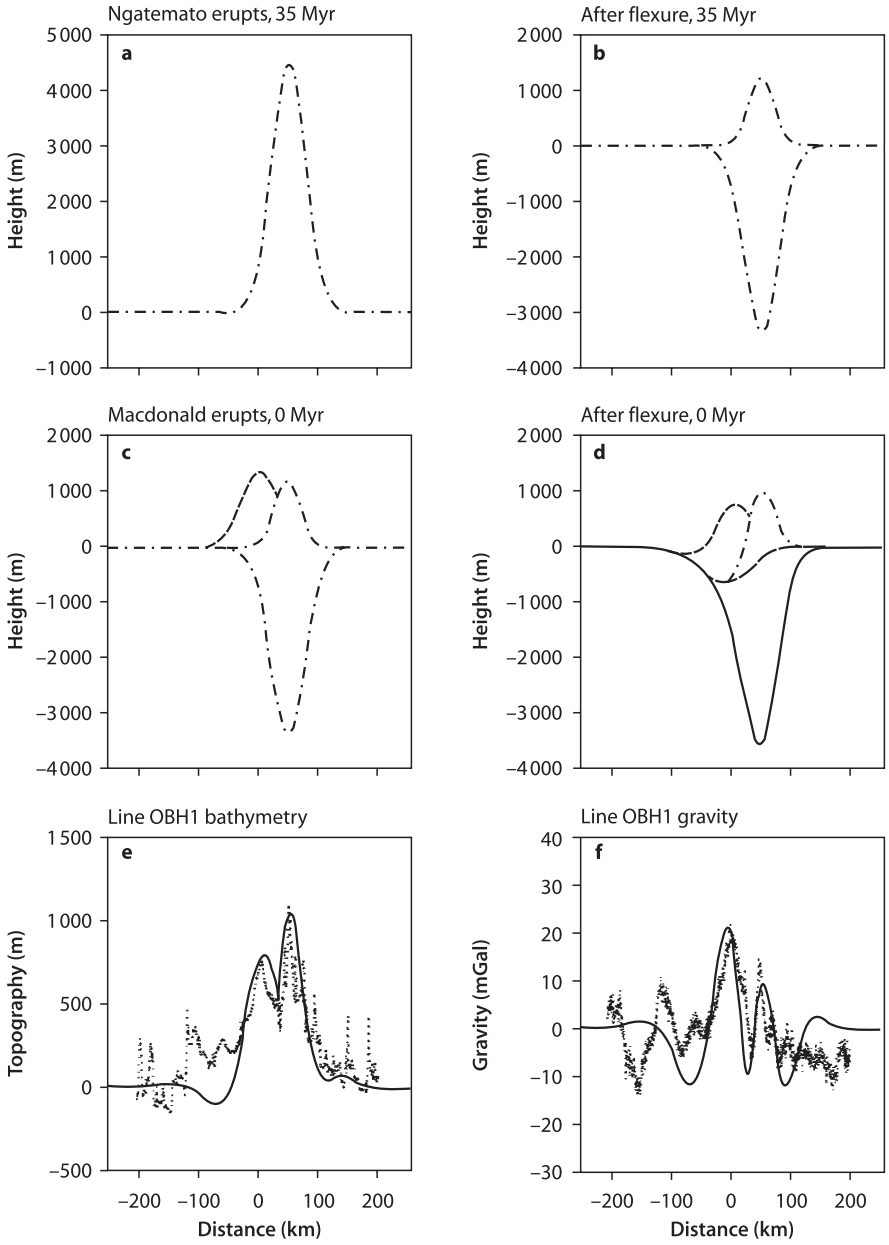

Fig. 1.14. Flexural modeling of lithospheric loading at two distinct times near Macdonald Seamount; **a** cross section showing load from older, near-ridge volcano erupting at 35 Ma; **b** net bathymetric profile resulting after load is compensated by flexure of a weak elastic plate; **c** smaller Macdonald Volcano erupts in the present; **d** net bathymetric profile after stiffer plate flexes to compensate the new, young load; **e** comparison of simple model bathymetry to multibeam data from the southern Austral Islands; **f** comparison of model gravity anomaly to the observed. From McNutt et al. (1997)

volcanic cones superimposed on one another (Fig. 1.11–1.13a and 1.13b). Apparently, these features are formed by a large number of discrete, small volcanoes forming in close proximity, presumably over a long period of time. The ridges that have been sampled and dated (Winterer and Sandwell 1997) show no evidence for a linear age progression along the feature and thus cannot be explained as hotspot features. The lack of age progression and the large-scale en échelon morphology suggests that these ridges result from lithospheric fractures that either tap ubiquitous upper mantle melt in the region or generate local decompression melting (Winterer and Sandwell 1997). Recent geochemical analyses also indicate that the Puka Puka lavas originated from the shallow upper mantle rather than from a hotspot (Janney et al. 2000). The morphological similarity of these en échelon ridge systems at both small and large scales suggests they may share a common origin.

High quality bathymetric data has also proved critical to calibrating the elastic thickness of the lithosphere (Filmer et al. 1993). As a good example, an initial estimate of the effective elastic plate thickness of Macdonald Seamount was 0 km (Calmant 1987; Calmant and Cazenave 1986), which is unexpectedly low considering that it is an active volcano resting on 43 Ma lithosphere. However, higher-resolution bathymetric surveys undertaken in the region of the Austral Islands demonstrated that Macdonald has recently erupted in the region of much older volcanoes (McNutt et al. 1997). The gravity signal used to calibrate the plate stiffness was measuring an average of the very low elastic thickness associated with the older volcanoes that erupted near the spreading center and the current, larger elastic thickness (15 km) associated with Macdonald (Fig. 1.14). While retaining the resolution of the multibeam data embedded in the context of the spline interpolation and single-beam sonar data, the new map presented in Fig. 1.3 should prove very useful for flexure studies.

Detailed analysis of multibeam bathymetry of the sea floor around Society and Austral Islands has also shown evidence of more than thirty-six submarine landslides (see Sect. 6.2.2 and 6.7). This inventory shows an evolution of the landslide type with the age of oceanic islands. Submarine active volcanoes are subject to superficial landslides of fragmental material, whereas young islands exhibit marks of mass wasting corresponding to giant lateral collapses due to debris-producing avalanches that occurred during the period of volcanic activity.

1.4 Conclusions

Bathymetric observations form the basis of nearly all geological, geophysical, and geomorphological studies of the sea floor. Unfortunately, we lack high quality bathymetry for vast areas of the sea floor, including most of French Polynesia. What data do exist are generally of uneven quality in terms of accuracy, resolution, and navigation. Furthermore, until now, there has not been one source of bathymetry data for French Polynesia that is comprehensive and in a common format. In producing the new data base and maps presented here, we have attempted to retain the information content in the original soundings, while still presenting the data at a large enough scale to be useful for regional synthesis. Our goal is to stimulate more studies of the sea floor of French Polynesia by making the highest quality data readily available.

Acknowledgements

The data synthesis efforts of Jordahl, Caress, and McNutt have been supported by the Packard Foundation. Development and support of MB-System is supported by the National Science Foundation and the Packard Foundation. Part of the database has been made available by the ZEPOLYF program funded by the French government and by the local government of French Polynesia. The authors particularly wish to acknowledge the work of all the scientists and crews involved in the expeditions that collected the data presented in this study.

References

Auzende JM, Bonneville A, Grandperrin R, Le Visage C (1997) Les programmes ZoNéCo et ZEPOLYF: Inventaire des zones économiques des Territoires Français du Pacifique, Marine Benthic Habitats. ORSTOM/IFREMER, Nouméa, pp 8

Bemis KG, Smith DK (1993) Production of small volcanoes in the Superswell region of the South Pacific. Earth Planet Sc Lett 118:251–262

Binard N, Hekinian R, Cheminée JL, Searle RC, Stoffers P (1991) Morphological and structural studies of the Society and Austral hotspot regions in the South Pacific. Tectonophysics 186(3–4):293–312

Bonneville A, Le Suavé R, Audin L, Clouard V, Dosso L, Gillot PY, Hildenbrand A, Janney P, Jordahl K, Keitapu M (2002) Arago Seamount: The Missing Hot Spot found in the Austral Islands. Geology 30:1023–1026

Calmant S (1987) The elastic thickness of the lithosphere in the Pacific Ocean. Earth Planet Sc Lett 85:277–288

Calmant S, Cazenave A (1986) The effective elastic lithosphere under the Cook Austral and Society Islands. Earth Planet Sc Lett 77:187–202

Calmant S, Cazenave A (1987) Anomalous elastic thickness of the oceanic lithosphere in the South Central Pacific. Nature 328:236–238

Cande SC, Haxby WF (1991) Eocene propagating rifts in the southwest Pacific and their conjugate features on the Nazca plate. J Geophys Res 96:19609–19622

Caress DW, Chayes DN (1996) Improved processing of Hydrosweep DS multibeam data on the R/V Maurice Ewing. Mar Geophys Res 18:631–650

Caress DW, McNutt MK, Detrick RS, Mutter JC (1995) Seismic imaging of hotspot-related crustal underplating beneath the Marquesas Islands. Nature 373:600–603

Cazenave A, Thoraval C (1993) Degree 6 upper mantle tomography and the south Pacific superswell. Earth Planet Sc Lett 57:63–74

Cazenave A, Thoraval C (1994) Mantle dynamics constrained by degree 6 surface topography, seismic tomography and geoid: Inference on the origin of the South Pacific Superswell. Earth Planet Sc Lett 122:297–219

Clouard V, Bonneville A, Gillot PY (2003) The Tarava Seamounts: A newly characterized hotspot chain on the South Pacific Superswell. Earth Planet Sc Lett 207(1–4):117–130

Courtney RC, White RS (1986) Anomalous heat flow and geoid across the Cape Verde Rise; Evidence for dynamic support from a thermal plume in the mantle. Geophys J Roy Astron Soc 87:815–867

Crough ST (1978a) Thermal origin of mid-plate hotspot swells. Geophys J Roy Astron Soc 55:451–469

Crough ST (1978b) Thermal origin of mid-plate, hot-spot swells. Eos Transactions American Geophysical Union 59(4), pp 270

Crough ST (1983) Hotspot swells. Annu Rev Earth Planet Sc Lett 11:165–193

Detrick RS, Crough ST (1978) Island subsidence, hotspots, and lithospheric thinning. J Geophys Res 83:1236–1244

Detrick RS, Von Herzen RP, Crough ST, Epp D, Fehn U (1981) Heat flow on the Hawaiian swell and lithospheric reheating. Nature 292:142–143

Duncan RA, McDougall I (1974) Migration of volcanism with time in the Marquesas Islands, French Polynesia. Earth Planet Sc Lett 21:414–420

Duncan RA, McDougall I (1976) Linear volcanism in French Polynesia. J Volcanol Geotherm Res 1: 197–227

Filmer PE, McNutt MK, Wolfe CJ (1993) Elastic thickness of the lithosphere in the Marquesas and Society Islands. J Geophys Res B 98:19565–19577

Janney PE, Macdougall JD, Natland JH, Lynch MA (2000) Geochemical evidence from the Pukapuka Volcanic ridge system for a shallow enriched mantle domain beneath the South Pacific Superswell, Earth Planet Sc Lett 181:47–60
Jordan TH (1979) Mineralogies, densities, and seismic velocities of garnet lherzolites and their geophysical implications. The Mantle sample: Inclusions in Kimberlites and other volcanics 2:1–14
Jordahl K, McNutt MK, Webb HW, Kruse SE, Kuykendall MG (1995) Why there are no earthquakes on the Marquesas Fracture Zone. J Geophys Res 100:24431–24447
Jordahl K, McNutt M, Buhl P (1997) Volcanism in the southern Austral Islands; time history, tectonic control, and large landslide events. Eos Transactions American Geophysical Union 78(46) Suppl, pp 720
Jordahl KA, McNutt M, Zorn H (1998) Pacific-Farallon relative motion 42–59 Ma determined from magnetic and tectonic data from the southern Austral Islands. Geophys Res Lett 25:2869–2872
Kuykendall MG, Kruse SE, McNutt MK (1994) The effect of changes in plate motions on the shape of the Marquesas Fracture Zone. Geophys Res Lett 21:2845–2848
Levitt DA, Sandwell DT (1996) Modal depth anomalies from multibeam data bathymetry: Is there a South Pacific Superswell? Earth Planet Sc Lett 139:1–16
Marty JC, Cazenave A (1989) Regional variations in subsidence rate of oceanic plates: A global analysis. Earth Planet Sc Lett 94:301–315
McNutt MK (1987) Temperature beneath the midplate swells: the inverse problem. In: Keating B, Fryer P, Batiza R, Boethlert G (eds) Seamounts, islands and atolls. Geophys Monogr AGU, pp 123–132
McNutt MK (1998) Superswells. Rev Geophys 36:211–244
McNutt MK, Bonneville A (2000) A shallow, chemical origin for the Marquesas swell. Geochemistry Geophysics Geosystems 1
McNutt MK, Fischer KM (1987) The south Pacific Superswell. In: Keating B, Fryer P, Batiza R, Boethlert G (eds) Seamounts, islands and atolls. Geophys Monogr AGU, pp 25–34
McNutt MK, Judge AV (1990) The superswell and mantle dynamics beneath the south Pacific. Science 248:969–975
McNutt MK, Sichoix L, Bonneville A (1996) Modals depths from shipboard bathymetry: There IS a South Pacific Superswell. Geophys Res Lett 23:3397–3400
McNutt MK, Caress DW, Reynolds J, Jordahl KA, Duncan RA (1997) Failure of plume theory to explain midplate volcanism in the Southern Austral Islands. Nature 389:479–482
Menard HW (1964) Marine geology of the Pacific. International series in the earth sciences. McGraw-Hill, New York, pp 271
Menard HW, McNutt MK (1982) Evidence and consequence of thermal rejuvenation. J Geophys Res 87:857
Monnereau M, Cazenave A (1990) Depth and geoid anomalies over oceanic hotspot swells: A global survey. J Geophys Res 95:15429–15438
N.G.D.C. (1988) National Geophysics Data Center, ETOPO5 bathymetry/topography data. Data announc. 88-MGG-02. National Oceanic and Atmospheric Administration, U.S. Department of Commerce, Boulder, CO
Nishimura CE, Forsyth DW (1985) Anomalous Love-wave phase velocitieis in the Pacific: Sequential pure-path and spherical harmonic inversion. Geophysical J Roy Astronom Soc 81:389–407
Okal EA, Cazenave J (1985) A model for the plate tectonic evolution of the east-central Pacific based on Seasat investigations. Earth Planet Sc Lett 72:99–116
Phipps MJ, Morgan WJ, Price E (1995) Hotspot melting generates both hotspot volcanism and hotspot swell? J Geophys Res 100:8045–8062
Robinson EM, Parsons B (1988a) Effect of a shallow low-viscosity zone on the formation of midplate swells. J Geophys Res 93:3144–3156
Sandwell DT (1984) Thermomechanical evolution of oceanic fracture zones. J Geophys Res 95 89: 11401–11413
Sandwell DT, Schubert G (1982) Lithospheric flexure at fracture zones. J Geophys Res 95 89:4657–4667
Sandwell DT, et al. (1995) Evidence for diffuse extension of the Pacific plate from Pukapuka Ridges and Cross-Grain gravity lineations. J Geophys Res 95 100:15087–15099
Scheirer DS, Macdonald KC, Forsyth DW, Shen Y (1996) Abundant seamounts of the Rano Rahi Seamount field near the Southern East Pacific Rise, 15 degrees S to 19 degrees S. Marine Geophys Res 18:13–52
Sichoix L, Bonneville A (1996) Prediction of bathymetry in French Polynesia constrained by shipboard data. Geophys Res Lett 23:2469–2472
Smith WHF, Sandwell DT (1994) Bathymetric prediction from dense satellite altimetry and sparse shipboard bathymetry. J Geophys Res 95 99:21803–21824
Smith WHF, Wessel P (1990) Gridding with continuous curvature splines in tension. Geophysics 55: 293–305

ten Brink US (1991) Volcano spacing and plate rigidity. Geology 19:397–400
Vogt PR (1974) Volcano spacing, fractures, and thickness of the lithosphere. Earth Planet Sc Lett 21: 235–252
Wessel P (2002) GMT Geoware CD-ROM vol. 1 version 1.2
Wessel P, Haxby WF (1990) Thermal stresses, differential subsidence, and flexure at oceanic fracture zones. J Geophys Res 95:375–391
Wessel P, Smith WHF (1996) A global self-consistent, hierarchical, high-resolution shoreline database. J Geophys Res 101:8741–8743
Winterer EL, Sandwell DT (1987) Evidence from en-echelon crossgrain ridges for tensional cracks in the Pacific plate. Nature 329:534–537
ZEPOLYF (1996a) Exploration de la zone Economique de Polynésie Française. Université du Pacifique – SMA – Ifremer – Ostom – Shom, Papeete – Tahiti
ZEPOLYF (1996b) Rapport de mission de la campagne ZEPOLYF-1. Université Française du Pacifique and IFREMER, Papeete – Tahiti

http://www.springer.com/978-3-540-40859-8

Oceanic Hotspots
Intraplate Submarine Magmatism and Tectonism
Hekinian, R.; Stoffers, P.; Cheminée, J.-L. (Eds.)
2004, XVI, 480 p., Hardcover
ISBN: 978-3-540-40859-8